# Pressure Behavior of Partially Penetrating Multiple Hydraulic Fractures

S. Al Rbeawi<sup>1</sup> & D. Tiab<sup>1</sup>

<sup>1</sup> Mewbourne School of Petroleum & Geological Engineering, University of Oklahoma, Norman, USA

Correspondance: S. Al Rbeawi, Mewbourne School of Petroleum & Geological Engineering, University of Oklahoma, 100 East Boyd St. Norman, OK, 73019, USA. Tel: 1-405-600-4907. E-mail: salam@ou.edu

Received: February 1, 2012Accepted: February 14, 2012Online Published: May 29, 2012doi:10.5539/eer.v2n1p244URL: http://dx.doi.org/10.5539/eer.v2n1p244

## Abstract

Horizontal wells with multiple hydraulic fractures have become a common occurrence in the oil and gas industry, especially in tight formations. Published models assume that hydraulic fractures are fully penetrating the formations. However, studies have shown that fractures are not always fully penetrating the formations.

This paper introduces a new technique for analyzing the pressure behavior of a horizontal well with multiple vertical and inclined partially penetrating hydraulic fractures. The hydraulic fractures in this model could be longitudinal or transverse, vertical or inclined, symmetrical or asymmetrical. The fractures are propagated in isotropic or anisotropic formations and considered having different dimensions and different spacing. This technique, based on pressure and pressure derivative concept, can be used to calculate various reservoir parameters, including directional permeability, fracture length and percentage of penetration. The study has shown that the pressure behavior of small penetration rate is similar to the horizontal wells without hydraulic fractures.

A type curve matching technique has been applied using the plots of the pressure and pressure derivative curves. A set of type curves, which will be included in the paper, have been generated for the partially penetrating hydraulic fractures associated to the horizontal wells with different penetration rates. A step-by-step procedure for analyzing pressure tests using these type curves is also included in the paper for several numerical examples.

**Keywords:** reservoir engineering, reservoir characterization, reservoir mathematical modeling, hydraulically fractured formation, well test analysis, pressure transient analysis

#### 1. Introduction

Several factors control the final output of the hydraulic fracturing process. Fracture dimensions (half fracture length, fracture width, and fracture height) are of great importance in the performance as are the orientation of the fractures as well as the rock and fluid properties. Typically, it is preferred that the fracture height be equal to the formation height, where fully-penetrating fractures can be produced. Unfortunately, the fractures can not always penetrate totally the formation where partially penetrating fractures may be produced. Partially penetrating hydraulic fractures are undesirable stimulation process due to the possibility of reducing the expected production rate of the fractured formation. However, fully penetrating fractures in a reservoir with water and oil in contact may lead to an early or immediate water production. Therefore, partially penetrating fractures may be the only way to prevent the production of unwanted water.

Great attentions have been focused to model the pressure transient behavior for either horizontal or vertical wells, with or without hydraulic fractures. As a result several models were developed based on the using of the source solution and Green's function to solve unsteady-state flow problem in the reservoir. Gringarten and Ramey (1973) used source function and Newman product method for solving transient flow problem. Although this approach is extremely powerful in solving two and three dimensions problem, it has some limitations such as incorporating the influence of storage and skin effects. The transient flow solutions have been extended to predict the behavior of the infinite conductivity vertical fracture in homogenous formations or in dual-porosity media. Ozkan (1988) presented an extensive library of different solutions for diffusivity equation in terms of the Laplace transform variable to reduce the limitations in the source solution presented by Gringarten and Ramey.

He considered a wide variety of wellbore configurations, different bounded systems, and homogeneous or double-porosity reservoirs.

Benjamin (1978) used a finite element model to study pressure behavior of a well intersecting a vertical fracture at the center of closed square reservoir. Wong et al (1985) analyzed the data using type curve matching and pressure and pressure derivative for cases of vertical fractured wells with no skin and no wellbore storage and cases with both skin and wellbore storage during the bi-linear flow period. Cinco-Ley and Meng (1988) studied the results obtained from the transient behavior of a well intersected by a vertical fracture in a double porosity reservoir. They introduced two models; the first one was a general semi-analytical and the second one was a simplified fully analytical model

Raghavan et al. (1997) developed a mathematical model to discern the characteristic response of multiply-fractured horizontal wells. Three significant flow periods have been observed based on their model; the early time period in which the system behaved like the one with n-layers, the intermediate time period in which the system reflected the interference between the fractures, and late time period in which the system behaved as a single fracture horizontal well with length equal the distance between the outermost fractures.

Wan and Aziz (1999) developed general solution for horizontal wells with multiple fractures. They showed that four flow regimes can be observed; the early linear, transient, late linear, and late time radial flow. Zerzar et al. (2003) combined the boundary element method and Laplace transformation to present a comprehensive solution for multiple vertical fractures horizontal wells. Seven flow regimes have been noticed; bilinear, first linear, elliptical, radial, pseudo-radial, second linear, and pseudo-steady state. Al-Kobaisi and Ozkan (2004) presented a hybrid numerical-analytical model for the pressure transient response of horizontal wells intercepted by a vertical fracture. Anh and Tiab (2009) solved the analytical model presented by Cinco-Ley (1974) for the pressure transient behavior caused by an inclined fracture associated with vertical wellbore. The model used the uniform flux and infinite conductivity fracture solution for different inclination angles from the vertical direction. Both type curve and TDS technique have been used to estimate the formation parameters such as permeability, skin factor, and fracture length.

Eventhouth, great attentions were focused on the study of pressure transient analysis of hydraulically fractured wells; there are few studies about the effects of the partially penetrating fractures. Raghavan et al (1978) were the first presented an analytical model that examines the effect of the fracture height on the pressure behavior of single vertical fracture. Their model was derived based on the solution technique presented by Gringarten and Ramey (1973). Rodriguez and Cinco-Ley (1984) developed semi-analytical solution for the transient flow behavior of a reservoir with a well intersecting a partially-penetrating single vertical fracture of both finite and infinite conductivity cases. The results of this study explained that the flow behavior of partially penetrating fracture. Alpheous and Tiab (2008) studied the effect of the partial penetrating infinite conductivity hydraulic fractures on the pressure behavior of horizontal well extending in naturally fractured formation. They stated that the duration of early linear flow regime is a function of the hydraulic fractures height.

# 2. Mathematical Models

The analytical model for the pressure behavior of a horizontal well intersecting with partially penetrating multiple vertical and inclined hydraulic fractures can be derived based on the solution for the diffusivity equation in the porous media. The following facts would be important to be noticed:

- The flow from the reservoir to the wellbore sections between fractures is negligible as compared with the flow from the reservoir to the fracture plane.
- Fluid flows from the reservoir to the well through planar inclined and vertical fractures.
- A first approximation of the behavior of the system is the uniform flux fracture case. It is assumed that fluid enters the fractures at a uniform rate per unit area of the fracture face.

The following assumptions are important for the derivation of the model:

- 1- The reservoir is homogenous, having constant and uniform thickness with two impermeable layers at the top and bottom of the formation.
- 2- Constant porosity and permeability in each direction, but the formation is anisotropic.
- 3- Gravitational and frictional effects are negligible.
- 4- The well is extending in the midpoint of the formation height (symmetrical).

- 5- Single phase fluid of small and constant compressibility, constant viscosity, and formation volume factor, flows from the reservoir to the wellbore.
- 6- Reservoir pressure is initially constant.

$$P\Big|_{t=0} = P_i \tag{1}$$

7- The pressure at the outer boundaries of the reservoir is assumed to be constant and equal to the initial reservoir pressure.

$$P_e = P_i \tag{2}$$

8- The pressure at the upper and lower impermeable boundaries is assumed to be constant so that:

$$\left. \frac{\partial P}{\partial Z} \right|_{Z=0} = 0 \tag{3}$$

$$\frac{\partial P}{\partial Z}\Big|_{Z=h} = 0 \tag{4}$$

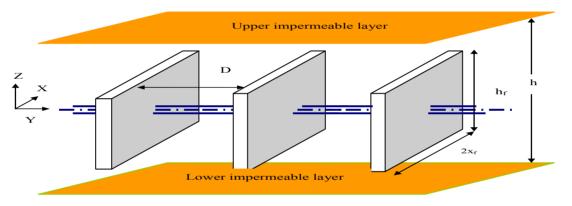


Figure 1. Horizontal well intersected by partially penetrating multiple vertical hydraulic fractures

Consider a horizontal well with partially penetrating vertical transverse hydraulic fractures in an infinite, homogenous, isotropic or anisotropic, horizontal slab reservoir as shown in Figure 1. Each fracture is considered as a single plane of length  $(2x_f)$ , width (w), height  $(h_f)$ . The spacing between fractures is (D). If we assume that all fluid withdrawal will be through the fractures, the fractures are partially penetrating the formation, the fractures can be simulated as inclined plane sources. The unsteady state pressure drop created by these planes at any point  $(x_m, y_m, z_m is:$ 

$$P(x_m, y_m, z_m, t, z_f, h_f, x_f, h) = \frac{q}{\phi c} \int_0^t S_{xyz}(x_m, y_m, z_m, t - \tau, z_f, h_f, x_f, h) d\tau$$
(5)

The model for pressure response of horizontal wells intersecting by multiple partially penetrating vertical hydraulic fractures in dimensionless form is:

$$P_{D} = \frac{\sqrt{\pi}}{4n} \int_{0}^{t_{D}} \frac{1}{\sqrt{t_{D}}} \left[ erf\left(\frac{x_{D}+1}{2\sqrt{t_{D}}}\right) - erf\left(\frac{x_{D}-1}{2\sqrt{t_{D}}}\right) \right] \times \sum_{n=1}^{n=\infty} e^{-\frac{(y_{D}-nD_{D})^{2}}{4t_{D}}} \times \left[ 1 + \frac{4}{\pi h_{hfD}} \sum_{N=1}^{N=\infty} \frac{1}{N} e^{-N^{2}\pi^{2}h_{hfD}^{2}t_{D}} \sin\left(N\pi \frac{h_{hfD}}{2}\right) \cos\left(N\pi z_{hfD}\right) \cos\left(N\pi z_{hfD}\right) \right] dt$$
(6)

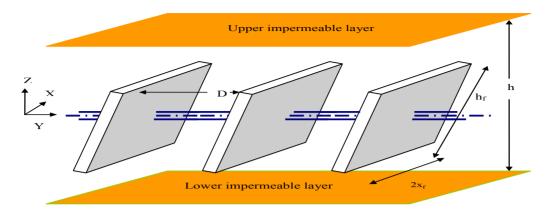


Figure 2. Horizontal well intersected by partially penetrating multiple inclined hydraulic fractures

For partially penetrating multiple inclined fractures as shown in Figure 2, the model for pressure behavior in dimensionless form is:

$$P_{D} = \frac{\sqrt{\pi}}{4n} \int_{0}^{t_{D}} \frac{1}{\sqrt{t_{D}}} \left[ erf\left(\frac{x_{D}+1}{2\sqrt{t_{D}}}\right) - erf\left(\frac{x_{D}-1}{2\sqrt{t_{D}}}\right) \right] \times \sum_{n=1}^{n=\infty} e^{-\frac{(y_{D}-nD_{D})^{2}}{4t_{D}}} \times \left[ 1 + \frac{4}{\pi h_{h/D}\cos(\theta_{v})} \sum_{N=1}^{N=\infty} \frac{1}{N} e^{-N^{2}\pi^{2}h_{s/D}^{2}t_{D}} \sin\left(N\pi \frac{h_{h/D}\cos(\theta_{v})}{2}\right) \cos\left(N\pi z_{h/D}\right) \cos\left(N\pi z_{h/D}\right) \right] dt$$

$$(7)$$

#### 3. Pressure Behavior

The penetration ratio (the ratio of the fracture's height to the formation's height) has significant influence on the pressure behavior at the wellbore and flow regimes in the vicinity of the wellbore. A set of type-curve matching plots will be presented in this paper to reflect the compound effect of the penetration ratio, the number of fractures, the spacing between fractures as well as fracture dimensions and inclination angle from the vertical axis. Seven flow regimes may develop for different cases:

- First linear flow: At early time, reservoir fluid flows linearly and directly from the formation to the individual fractures in the XZ plane.
- Second Linear Flow: When the pressure pulse reaches the upper and lower boundary, reservoir fluid continues flowing linearly and directly from the formation to the fractures in the XZ plane.
- Third Linear Flow: This flow regime develops for short spacing, large number of hydraulic fractures and large half fracture length. In this case, pressure behavior can be considered similar to the pressure behavior of long horizontal wells.
- Early radial flow: Early radial flow regime represents the radial flow around each fracture in the YZ plane. Typically, this flow is observed when the penetration ratio is small ( $h_{hfD}$ <0.5) and the spacing between fractures is long ( $D_D$ >5).
- Intermediate radial flow: Intermediate radial flow regimes develop for long spacing between fractures when there is sufficient time for reservoir fluid to flow radially in the XY plan to each individual fracture.
- Pseudo-radial flow: Pseudo-radial flow regime is the dominant flow for all cases at late time when reservoir fluids flow in the XY plane radially toward the fractures.
- Elliptical flow: This flow regime indicates elliptical flow toward the fractures.

The following responses are easy to identify based on different penetration ratios and different half fracture lengths:

#### 3.1 Large Penetration Ratio ( $h_{hfD} > 0.5$ )

Because of the penetration ratio, the pressure behavior in this case tends to be similar to the fully penetrating fractures where other factors such as the number of fractures, spacing between them, fracture dimensions, and inclination angle have the main influence.

3.1.1 Short half Fracture Length ( $h_{xfD} < 10$ )

- 1) For a small number of hydraulic fractures (less than five) and short spacing, first linear, transition, second linear, transition and pseudo-radial flow are observed as shown in Figure 3 and Figure 4.
- 2) For a small number of hydraulic fractures (less than five) and long spacing, first linear, transition, second linear, intermediate radial, transition and pseudo radial flow are observed as shown in Figure 5 and Figure 6.
- 3) For a large number of hydraulic fractures (more than five) and small spacing, first linear flow, transition flow, second linear flow, third linear flow, transition flow, and pseudo-radial flow regimes are observed such as in Figure 7 and Figure 8.
- 4) For a large number of hydraulic fractures (more than five) and long spacing, first linear, transition, second linear, intermediate radial, elliptical, transition and pseudo radial flow regimes are observed as shown in Figure 9 and Figure 10.

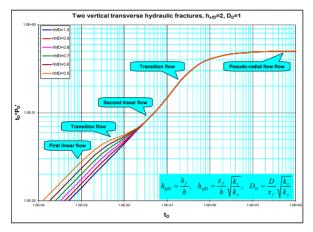


Figure 3. Pressure behavior of two partially penetrating vertical hydraulic fractures

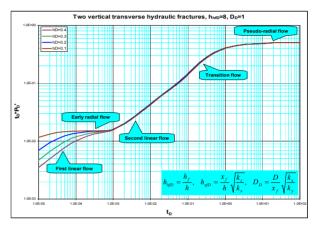


Figure 4. Pressure behavior of two partially penetrating vertical hydraulic fractures

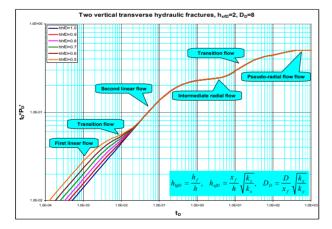


Figure 5. Pressure behavior of two partially penetrating vertical hydraulic fractures

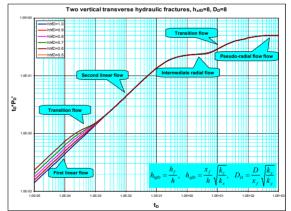


Figure 6. Pressure behavior of two partially penetrating vertical hydraulic fractures

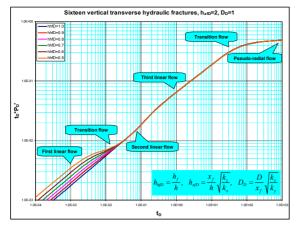


Figure 7. Pressure behavior of sixteen partially penetrating vertical hydraulic fractures

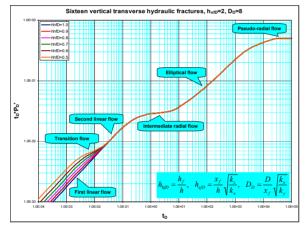


Figure 9. Pressure behavior of sixteen partially penetrating vertical hydraulic fractures

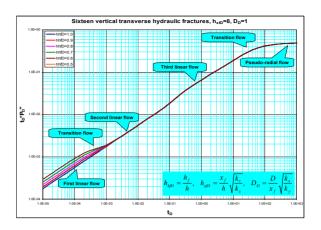


Figure 8. Pressure behavior of sixteen partially penetrating vertical hydraulic fractures

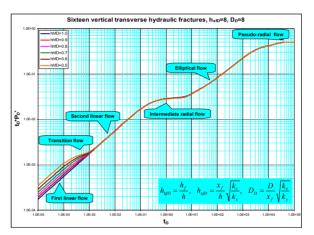


Figure 10. Pressure behavior of sixteen partially penetrating vertical hydraulic fractures

### 3.1.2 Long Half Fracture Length (hxfD>10)

- For a small number of hydraulic fractures (less than five) and short spacing, first linear flow, transition flow, second linear flow, transition flow, and pseudo-radial flow regimes are observed as shown in Figure 11 and Figure 12.
- 2) For a small number of hydraulic fractures (less than five) and long spacing, first linear flow, transition flow, second linear flow, intermediate radial flow, transition flow, and pseudo radial flow regimes are observed as shown in Figure 13 and Figure 14.
- 3) For a large number of hydraulic fractures (more than five) and small spacing, first linear flow is not observed. Therefore, second linear flow, third linear flow, transition flow, and pseudo-radial flow regimes are the only flow regimes that are observed such as in Figure 15 and Figure 16.
- 4) For a large number of hydraulic fractures (more than five) and long spacing, first linear flow also is not observed. Second linear flow, intermediate radial flow, elliptical flow, transition flow, and pseudo radial flow regimes are observed as shown in Figure 17 and Figure 18.

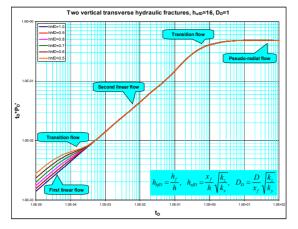


Figure 11. Pressure behavior of two partially penetrating vertical hydraulic fractures

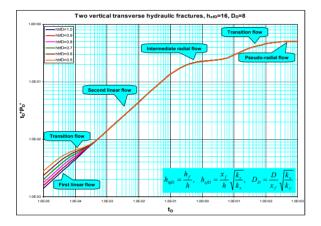


Figure 13. Pressure behavior of two partially penetrating vertical hydraulic fractures

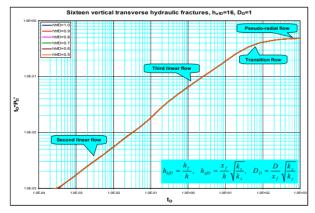


Figure 15. Pressure behavior of sixteen partially penetrating vertical hydraulic fractures

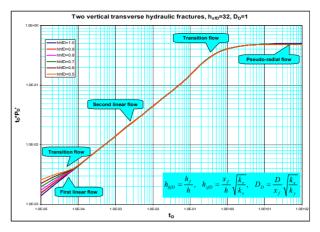


Figure 12. Pressure behavior of two partially penetrating vertical hydraulic fractures

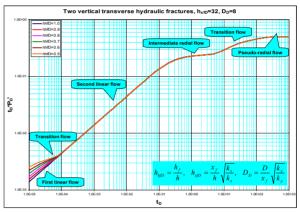


Figure 14. Pressure behavior of two partially penetrating vertical hydraulic fractures

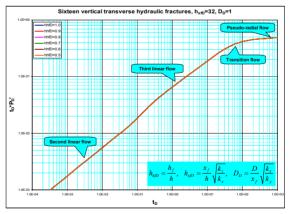


Figure 16. Pressure behavior of sixteen partially penetrating vertical hydraulic fractures

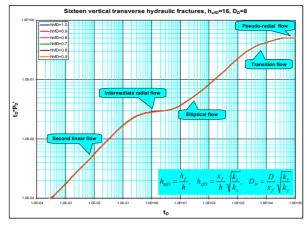


Figure 17. Pressure behavior of sixteen partially penetrating vertical hydraulic fractures

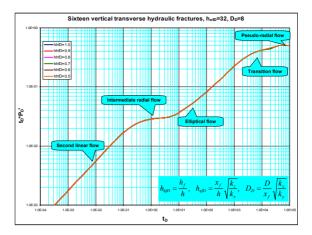


Figure 18. Pressure behavior of sixteen partially penetrating vertical hydraulic fractures

## 3.2 Small Penetration Ratio ( $h_{hfD} < 0.5$ )

Because of the small penetration ratio, the pressure behavior at early time tends to develop a new early radial flow regime where the flow of fluid takes place in the YZ plane.

3.2.1 Short Half Fracture Length ( $h_{xfD}$ <10)

- For a small number of hydraulic fractures (less than five) and short spacing, first linear flow, transition flow, early radial flow, second linear flow for h<sub>xfD</sub>>5, and transition flow for h<sub>xfd</sub><5, and pseudo-radial flow regimes are observed as shown in Figure 19 and Figure 20.</li>
- 2) 2- For a small number of hydraulic fractures (less than five) and long spacing, first linear flow, early radial flow, second linear flow, transition flow, intermediate radial flow, transition flow, and pseudo radial flow regimes are observed as shown in Figure 21 and Figure 22.
- 3) 3- For a large number of hydraulic fractures (more than five) and small spacing, first linear flow, early radial flow, second linear flow, third linear flow, transition flow, and pseudo-radial flow regimes are observed for  $h_{xfD}$ <5 such as in Figure 23. While for  $h_{xfD}$ >5, first linear flow can not be observed such as in Figure 24.
- 4) 4- For a large number of hydraulic fractures (more than five) and long spacing, first radial flow, early radial flow, second linear flow, intermediate radial flow, elliptical flow, transition flow, and pseudo radial flow regimes are observed for h<sub>xfD</sub><5 as shown in Figure 25. While for h<sub>xfD</sub>>5, first linear flow can not be observed as shown in Figure 26.

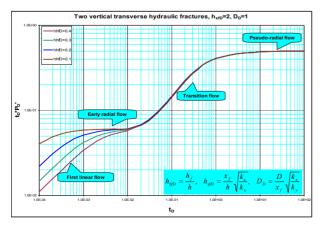


Figure 19. Pressure behavior of two partially penetrating vertical hydraulic fractures

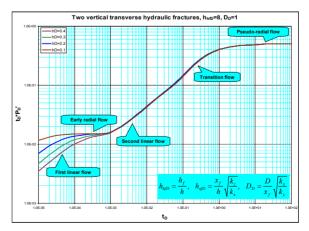


Figure 20. Pressure behavior of two partially penetrating vertical hydraulic fractures

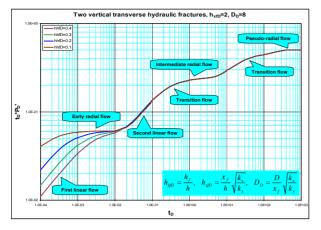


Figure 21. Pressure behavior of two partially penetrating vertical hydraulic fractures

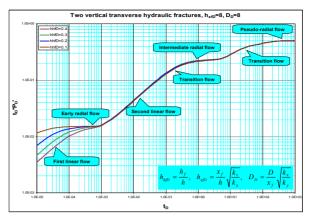


Figure 22. Pressure behavior of two partially penetrating vertical hydraulic fractures

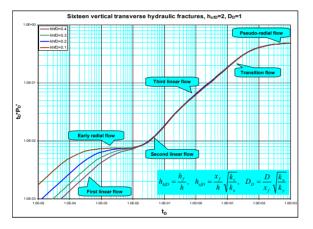


Figure 23. Pressure behavior of sixteen partially penetrating vertical hydraulic fractures

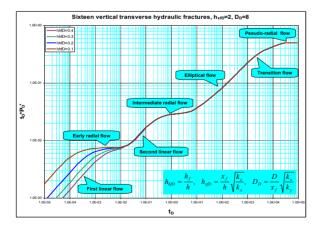


Figure 25. Pressure behavior of sixteen partially penetrating vertical hydraulic fractures

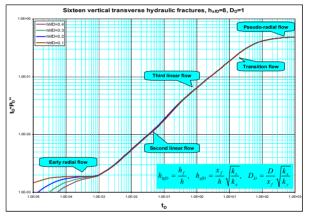


Figure 24. Pressure behavior of sixteen partially penetrating vertical hydraulic fractures

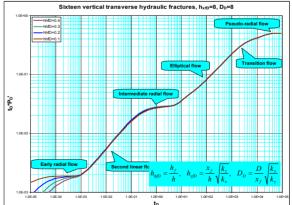


Figure 26. Pressure behavior of sixteen partiallypenetrating vertical hydraulic fractures

3.2.2 Long Half Fracture Length (hxfD>10)

- 1) For a small number of hydraulic fractures (less than five) and short spacing, first linear flow can not be observed. Early radial flow, second linear flow, transition flow, and pseudo-radial flow regimes are observed as shown in Figure 27 and Figure 28. The behavior in these two cases is similar to horizontal wells with short to moderate wellbore length.
- 2) For a small number of hydraulic fractures (less than five) and long spacing, first linear flow can not be observed. Early radial flow, second linear flow, transition flow, intermediate radial flow, transition flow, and pseudo radial flow regimes are observed as shown in Figure 29 and Figure 30.
- 3) For a large number of hydraulic fractures (more than five) and small spacing, neither first linear flow nor early radial flow can be observed. Second linear flow, third linear flow, transition flow, and pseudo-radial flow are the only flow regimes that are observed such as in Figure 31 and Figure 32. The behavior in these two cases is similar to a single vertical hydraulic fracture.
- 4) For a large number of hydraulic fractures (more than five) and long spacing, neither first linear flow nor early radial flow can be observed also. Second linear flow, intermediate radial flow, elliptical flow, transition flow, and pseudo radial flow regimes are observed as shown in Figure 33 and Figure 34. The behavior in these two cases is similar to multiple hydraulic fractures.

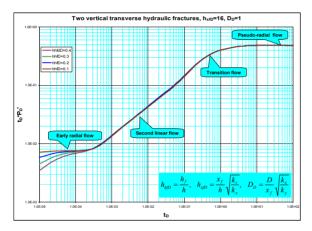


Figure 27. Pressure behavior of two partially penetrating vertical hydraulic fractures

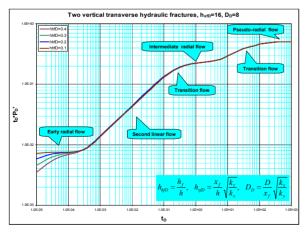


Figure 29. Pressure behavior of two partially penetrating vertical hydraulic fractures

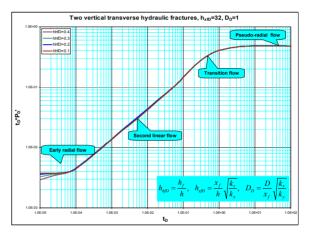


Figure 28. Pressure behavior of two partially penetrating vertical hydraulic fractures

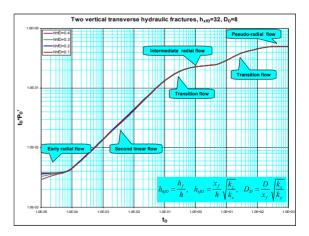


Figure 30. Pressure behavior of two partially penetrating vertical hydraulic fractures

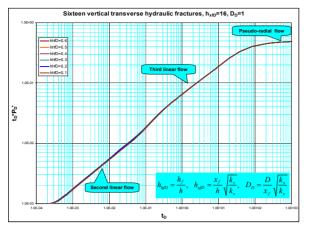


Figure 31. Pressure behavior of sixteen partially penetrating vertical hydraulic fractures

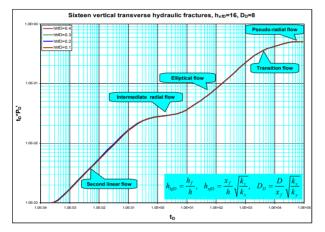


Figure 33. Pressure behavior of sixteen partially penetrating vertical hydraulic fractures

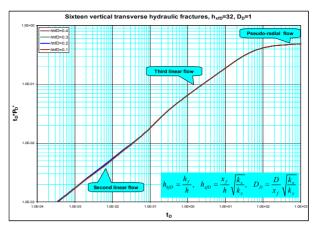


Figure 32. Pressure behavior of sixteen partially penetrating vertical hydraulic fractures

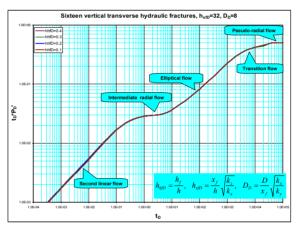


Figure 34. Pressure behavior of sixteen partially penetrating vertical hydraulic fractures

# 4. Effect of Inclination Angle

The inclination angle from the vertical axis  $(\theta_v)$  has a similar effect on pressure behavior of partially penetrating hydraulic fractures as the penetration ratio. It can be explained by the reduction in the fracture height which produces a reduction in the penetration ratio, when the fractures are inclined from the vertical direction. As fractures propagate in inclined directions rather than the vertical one, the probability for partially penetrating fractures to occur is reasonable. Figure 35 and Figure 36 represent pressure behaviors for two partially penetrating inclined hydraulic fractures for different inclination angles. While Figure 37 and Figure 38 represent pressure behaviors of ten partially penetrating inclined hydraulic fractures for different inclination angles. For all cases, the early radial flow develops when the inclination angle from the vertical direction increases.

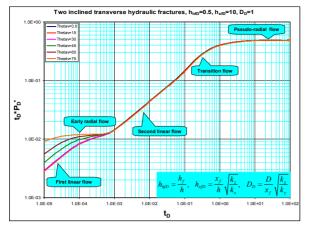


Figure 35. Pressure behavior of two partially penetrating inclined hydraulic fractures

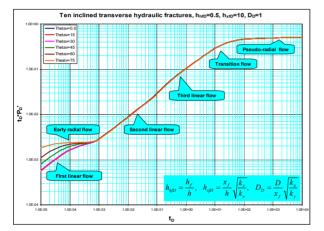


Figure 37. Pressure behavior of ten partially penetrating inclined hydraulic fractures

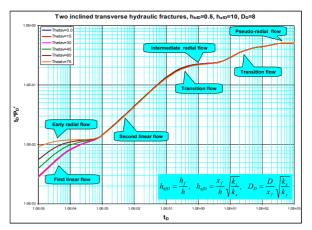


Figure 36. Pressure behavior of two partially penetrating inclined hydraulic fractures

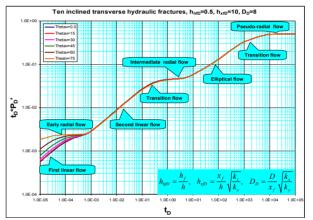


Figure 38. Pressure behavior of ten partially penetrating inclined hydraulic fractures

# 5. Application of Type Curve Matching

As shown on the plots in Appendix (B), the pressure and pressure derivative have different shapes for each combination of penetration rate, half fracture length, number of fractures, spacing between fractures, and inclination angle from the vertical axis. Type-curve matching can provide a quick estimation for reservoir and fractures parameters.

The following information is associated with each type curve: penetration rate ( $h_{hfD}$ ), half fracture length to fracture height ratio ( $h_{xfD}$ ), dimensionless spacing between fractures ( $D_D$ ), number of fractures (n), and inclination angle ( $\phi_v$ ). Thus, the following information can be obtained from the type curve matching process: ( $P_D$ )<sub>M</sub>, ( $\Delta P$ )<sub>M</sub>, ( $t_D$ )<sub>M</sub>, ( $\Delta t$ )<sub>M</sub>, ( $\phi_v$ )<sub>M</sub>, ( $h_{xfD}$ )<sub>M</sub>, (D)<sub>M</sub>, ( $h_{hfD}$ )<sub>M</sub>, (n)<sub>M</sub>. The following steps illustrate how type curve matching is used to determine reservoir characteristics such as: permeability, inclination angle, spacing, pseudo-skin factor, fracture half length, and number of fractures.

**Step-1** Plot ( $\Delta P$  vs. t) and ( $t \times \Delta P'$  vs. t) on log-log paper.

Step-2 Obtain the best match of the data with one of the type curves.

**Step-3** Read from any match point:  $t_M$ ,  $\Delta P_M$ ,  $t_{DM}$ ,  $P_{DM}$ ,  $h_{hxfDM}$ ,  $D_{DM}$ ,  $\phi_{vM}$ ,  $n_M$ ,  $h_{hfDM}$ . **Step-4** Calculate  $k_x$ :

$$k_{x} = \frac{\phi \mu c_{t} x_{f}^{2} t_{DM}}{0.0002637 t_{M}}$$
(8)

**Step-5** Calculate (*k<sub>y</sub>*):

$$k_{y} = \frac{1}{k_{x}} \left[ \frac{141.2quBP_{DM}}{h\Delta P_{M}} \right]^{2}$$
(9)

Step-6 Determine penetration ratio:

$$Penetration\ ratio = \frac{h_f}{h} = h_{hfDM}$$
(10)

Step-7 Calculate the height of fractures:

$$h_f = h_{h \not DM} \times h \tag{11}$$

Step-8 Calculate the half fracture length:

$$x_f = h_{xfDM} \times h \times \sqrt{\frac{k_x}{k_z}}$$
(12)

Step-9 Calculate the spacing between fractures:

$$D = D_{DM} \times x_f \sqrt{\frac{k_y}{k_x}}$$
(13)

Step-10 Number of fractures can be determined directly as:

$$n = n_M \tag{14}$$

Step-11 Inclination angle can be determined directly as:

$$\phi v = \phi_{vM} \tag{15}$$

#### 5.1 Example -1

Pressure drawdown test data of a hydraulically fractured horizontal well, extending in homogenous isotropic reservoir, is given in Table (Example C-1) of Appendix (C). Other known reservoir and well data are:

q = 500 STB/D	$\phi = 0.04, \ \mu = 0.5 \ cp$	$c_t = 1.0 \times 10^{-6} \text{ psi}^{-1}$	h = 40 ft
$r_w = 0.5 \text{ ft}$	p <sub>i</sub> = 5000 psi	B = 1.1  bbl/STB	

Determine:

1-Formation permeability.

2-Number of fractures.

3-Fracture half length.

4-Fracture height and penetration ratio.

5-Spacing between fractures.

6-Inclination angle.

## Solution

**Step-1** Plot ( $\Delta P$  vs. t) and ( $t \times \Delta P'$  vs. t) on log-log paper as shown in Figure 39.

Step-2 Obtain the best match of the data with one of the type curves as shown in Figure 40.

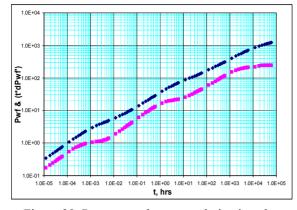


Figure 39. Pressure and pressure derivative plot Example -1

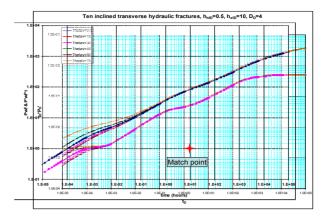


Figure 40. Type-curve matching plot for Example -1

Step-3 Read from any match point:

$$t_M = 10, \Delta P_M = 1, t_{DM} = 1.7, P_{DM} = 0.002, h_{hpDM} = 0.5, D_{DM} = 4, \phi_{vM} = 45, n_M = 10, s_M = -3.46, h_{xpDM} = 10, h_{xpDM}$$

**Step-4** Calculate half fracture length  $(x_f)$  from Equation 12.

$$x_f = 10 \times 40 = 400 \ ft$$

Step-5 Calculate *k* from Equation 8.

$$k = \frac{0.04 \times 0.5 \times 0.000001 \times 400^2 \times 1.7}{0.0002637 \times 10} = 2 \ md$$

Step-6 Number of fractures:

$$n = n_M = 10$$
 fractures

Step-7 Penetration ratio:

$$\frac{h_f}{h} = h_{hfD} = 0.5$$

Step-8 Calculate fracture height from Equation 11.

$$h_f = 0.5 \times 40 = 20 \ ft.$$

Step-9 Inclination angle:

 $\phi v = 45$ 

Step-10 Spacing between fractures from Equation 13.

$$D = x_f \times D_{DM} = 400 \times 4 = 1600 \ ft$$

Table 1 summarizes the input data and the resulted values of Example-1.

5.2 Example -2

Pressure drawdown test data of a hydraulically fractured horizontal well is given in Table (C-2) in Appendix (C). Sixteen vertical hydraulic fractures have been designed with a half fracture length (310 ft). Other known reservoir and well data are:

 $\begin{array}{ll} q = 100 \; STB/D & \varphi = 0.04 & \mu = 0.8 \; cp & c_t = 1.0 \times 10^{-6} \; psi^{-1} & h = 10 \; ft \\ r_w = 0.5 \; ft & p_i = 10000 \; psi & B = 1.1 \; bbl/STB \end{array}$ 

## Determine:

- 1-Formation permeabilities.
- 2-Fracture height and penetration ratio.
- 3-Spacing between fractures.

## Table 1. Summary of results of Example-1

Parameter In-put value		Calculated value by Type-curve matching technique
k, md	2	2
$x_{f}$ , ft	400	400
n	10	10
Penetrating ratio	0.5	0.5
<i>h<sub>f</sub></i> , ft	20	20
$ heta_{v}$	45	44
D, ft	1600	1600

# Solution

**Step-1** Plot ( $\Delta P$  vs. t) and ( $t \times \Delta P'$  vs. t) on log-log paper as shown in Figure 41. **Step-2** Obtain the best match of the data with one of the type curves as shown in Figure 42.

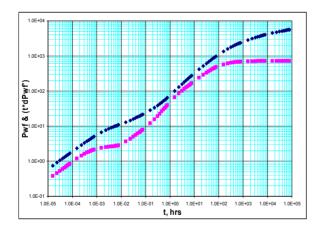


Figure 41. Pressure and pressure derivative plot Example -2

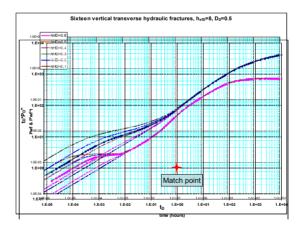


Figure 42. Type-curve matching plot for Example -2

Step-3 Read from any match point:

$$t_M = 1, \Delta P_M = 1, t_{DM} = 0.13, P_{DM} = 0.0007, h_{hfDM} = 0.3, D_{DM} = 0.5, n_M = 16, s_M = -2.09, h_{xfDM} = 8$$

**Step-4** Calculate  $k_x$  from Equation 8.

$$k_x = \frac{0.04 \times 0.8 \times 0.000001 \times 310^2 \times 0.13}{0.0002637 \times 1} = 1.5 \ md$$

**Step-5** Calculate  $(k_z)$  from Equation 12.

$$k_z = \left(\frac{8 \times 10}{310}\right)^2 \times 1.5 = 0.1 \, md$$

**Step-6** Calculate  $(k_y)$  from Equation 9.

$$k_y = \frac{1}{1.5} \left[ \frac{141.2 \times 100 \times 0.8 \times 1.1 \times 0.0007}{10 \times 1} \right]^2 = 0.5 \ md$$

Step-7 Number of fractures:

$$n = n_M = 16 \, fractures$$

Step-8 Penetration ratio:

$$\frac{h_f}{h} = h_{hfD} = 0.3$$

Step-9 Calculate fracture height from Equation 11.

$$h_f = 0.3 \times 10 = 3 ft.$$

Step-10 Spacing between fractures from Equation 13.

$$D = 310 \times 0.5 \times \sqrt{\frac{0.5}{1.5}} = 89.5 \ ft$$

Table-2 summarizes the input data and the resulted value for Example-2.

Table 2. Summary	of results	of Example-2
------------------	------------	--------------

Parameter	In-put value	Calculated value by type-curve matching
$k_x$ , md	1.5	1.5
$k_y$ , md	0.5	0.5
$k_z$ , md	0.1	0.1
Penetrating ratio	0.3	0.3
$h_{f}$ , ft	3	3
n	16	16
D, ft	89.5	89.5

#### 6. Conclusions

- An early radial flow regime is expected to be noticed for the case of the partially penetrating hydraulic fractures where the fluid flows radially in the parallel plane to the wellbore toward each individual fracture. This type of flow regime can be used as an indication for the uncompleted penetration or the fracture height is less than the formation height.
- 2) Second linear flow represents fluid's linear flow from the formation toward each fracture in the normal plane to the wellbore. This flow regime develops shortly after the upper and lower boundaries have been reached.
- 3) Third linear flow regime develops for short spacing partially penetrating hydraulic fractures where the fluid flows linearly in a parallel plane to the wellbore.

- 4) Intermediate radial flow appears for the case of wide spacing between fractures where the radial flow in the horizontal plane toward each fracture is developed. Intermediate radial flow can be used as an indication for serious production problem when the fractures do not perform properly.
- 5) For small penetrating ratio and large number of hydraulic fractures, the pressure behavior is similar to the behavior of long horizontal wells.
- 6) The inclination angle from the vertical direction has the same impact of the partial penetrating on pressure behavior of hydraulically fractured horizontal wells.

## Nomenclatures

В	formation volume factor	D	spacing between fractures, ft
h	formation height, ft	$h_{\mathrm{f}}$	fracture height, ft
$\mathbf{c}_{\mathrm{t}}$	total compressibility, psi <sup>-1</sup>	$\mathbf{k}_{\mathbf{x}}$	permeability in the X-direction, md
$\mathbf{k}_{\mathbf{y}}$	permeability in the Y-direction, md	$\mathbf{k}_{\mathbf{z}}$	permeability in the Z-direction, md
n	number of fractures	Ν	index
$\Delta P$	pressure difference		Q total flow rate, STB/D
q	fracture flow rate, STB/D	$r_w$	wellbore radius, ft
t	time, hrs	$x_{f}$	fracture half length, ft
Gree	k Symbols		

- $\phi$  porosity  $\mu$  viscosity, cp
- $\eta$  diffusivity  $\theta_v$  inclination angle from vertical direction

#### References

- Al-Kobaisi, M., & Ozkan, E. (2004). A hybrid numerical analytical model of finite conductivity vertical fractures intercepted by a horizontal well. SPE 92040 presented at SPE International Petroleum Conference in Puebla, Mexico, 8-9 Nov.
- Alpheus, O., & Tiab, D. (2008). Pressure Transient analysis in Partially penetrating Infinite Conductivity Hydraulic Fractures in naturally fractured Reservoirs. SPE 116733 presented at the SPE Annual Technical conference and Exhibition, Denver, Colorado, 21-24 September.
- Anh, V. Dinh, & Tiab, D. (2009a). Transient pressure analysis of a well with an inclined hydraulic fracture using Tiab's direct synthesis technique. SPE 120545 presented at SPE Production and Operation Symposium held in Oklahoma City, USA, 4-8 April.
- Anh, V. Dinh, & Tiab, D. (2009b). Transient pressure analysis of a well with an inclined hydraulic fracture using type curve matching. SPE 120540 presented at SPE Production and Operation Symposium held in Oklahoma City, USA, 4-8 April.
- Benjamin, J. (1978). Transient flow to finite conductivity fractures. SPE 7489 presented at the 53rd SPE Annual Technical Conference and Exhibition, 1-3 Oct., Dallas, TX.
- Cinco-Ley, H. (1974). Unsteady-State Pressure Distribution Created by a Slanted Well or a Well with an Inclined Fracture. PhD dissertation, Stanford University, California, May (1974).
- Cinco-Ley, H., & Samaniego. (1981). Transient Pressure Analysis: finite conductivity fracture case versus damaged fracture case SPE 10179 presented at the 56th Annual Fall Technical Conference and Exhibition, San Antonio, USA, 5-7 Oct.
- Cinco-Ley, H., & Z. Meng. (1988). Pressure transient analysis of wells with finite conductivity vertical fractures in double porosity reservoirs. SPE 18172 presented at the SPE 63rd Annual Technical Conference and Exhibition, Houston, TX, 2-5 Oct.
- Cinco-Ley, H., Ramey, H. J., & Miller, F. G. (1975). Unsteady-State Pressure Distribution Created by a Well with an Inclined Fracture. SPE 5591 presented at the 50th Annual Fall Meeting, Dallas, USA. 28 Sep.-1 Oct.
- Gringarten, A. C., & Ramey, H. J. (1973). The Use of Source and Green's Function in Solving Unsteady-Flow Problem in Reservoir. *SPE Journal*, 285-296, SPE 3818.
- Ozkan, E. (1988). Performance of horizontal wells. Ph.D. Dissertation, The University of Tulsa, May (1988).

- Raghavan, R., Chin-Cheng Chen, & Bijin Agarwal. (1997). An analysis of horizontal wells intercepted by multiple fractures. SPE Journal, SPE- 27652.
- Raghavan, R., Uraiet, A., & Thomas, G. (1978). Vertical Fracture Height: Effect on Transient Flow Behavior. SPE Journal, 268- 277, SPE 6016.
- Rodriguez, F, Horne, R., & Cinco-Ley, H. (1984). Partially Penetrating Fractures: Pressure Transient Analysis of an Infinite Conductivity Fracture. SPE 12743 presented at the SPE California Regional Meeting, Long Beach, CA, 11-13 April.
- Rodriguez, F, Horne, R., & Cinco-Ley, H. (1984). Partially Penetrating Fractures: Pressure Transient Analysis of a finite Conductivity Fracture. SPE 13057 presented at the 59th SPE Annual Technical Conference and Exhibition, Houston, Texas, 16-19 September.
- Slimani, K., & Tiab, D. (2006). Pressure Transient analysis of partially Penetrating Wells in a Naturally Fractured Reservoirs. SPE 104059 presented at the first International Oil Conference and Exhibition in Cancun, Mexico, 31 august-2 September.
- Tiab, D. (1993). Analysis of Pressure Derivative without Type-Curve Matching: Vertically Fractured Wells in Closed Systems. SPE 26138 presented at the SPE Western Regional Meeting, 26-28 May, Anchorage, Alaska.
- Tiab, D., & Puthigai, S. K. (1988). Pressure Derivative Type-Curves for a Vertically Fractured Well. SPEFE, 156-158, SPE 11028.
- Wan J., & K. Aziz. (1999). Multiple hydraulic fractures in horizontal wells. SPE 54627 presented at the SPE Western Regional Meeting, 26-28 May, Anchorage, Alaska.
- Wong, D., Harrington, A., & Cinco-Ley, H. (1986). application of the pressure derivative function in the pressure transient testing of fractured wells, SPE formation evaluation, 470-480, SPE 13056.
- Wright, C. A., & Conant, R. A. (1995). Hydraulic Fracture Reorientation in Primary and Secondary Recovery from Low Permeability Reservoirs. SPE 30484 presented at the SPE Annual Technical Conference, Dallas, USA, 22-25 Oct.
- Wright, C. A., Davis, Minner, W. A. E. J. et al. (1998). Surface Tiltmeter Fracture Mapping Reaches New Depths – 10000 Feet, and Beyond. SPE 39919 presented at SPE Rocky Mountain Regional/Low-Permeability Reservoir Symposium and Exhibition, Denver, USA, 5-8 April.
- Zerzar, A., Bettam, Y., & Tiab, D. (2003). Interpretation of multiple hydraulically fractured horizontal wells in closed systems. SPE 84888 presented at SPE International Improved Oil Recovery Conference in Asia Pacific, Kuala Lumpur, Malaysia, 20-21 Oct.

#### **Appendix-A: Models Derivation**

#### 1) Vertical Hydraulic Fractures:

Consider a horizontal well with partially penetrating vertical transverse hydraulic fractures in an infinite, homogenous, isotropic or anisotropic, horizontal slab reservoir as shown in Figure A-1. Each fracture is considered as a single plane of length  $(2x_f)$ , width (w), height  $(h_f)$ . The spacing between fractures is (D). If we assume that all fluid withdrawal will be through the fractures, the fractures are partially penetrating the formation, the fractures can be simulated as inclined plane sources. The unsteady state pressure drop created by these planes at any point  $(x_m, y_m, z_m)$  is:

$$P(x_m, y_m, z_m, t, z_f, h_f, x_f, h) = \frac{q}{\phi c} \int_0^t S_{xyz}(x_m, y_m, z_m, t - \tau, z_f, h_f, x_f, h) d\tau$$
(A-1)

where;

 $S_{xyz}$  is the instantaneous source function for an inclined plane source in an infinite slab reservoir and (q) is the fluid withdrawal per unit fracture surface area per unit time.

$$S_{xyz}(x_m, y_m, z_m, t, z_f, h_f, x_f, h) = S_x(x, t) \times S_y(y, t) \times S_z(z, t)$$
(A-2)

$$q = \frac{Q}{2nx_f h_f} \tag{A-3}$$

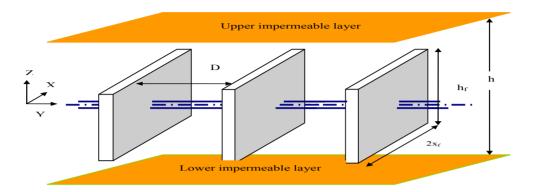


Figure A-1. Horizontal well intersected by partially penetrating multiple hydraulic fractures

 $S_x$  is the instantaneous source function for an infinite slab source in an infinite reservoir in the direction of X-axis.  $S_y$  is the instantaneous source function for an inclined plane source in an infinite slab reservoir in the Y-direction.  $S_z$  is the instantaneous source function for an inclined plane source in an infinite slab reservoir in the vertical direction as shown in Figure A-2.  $S_x$  can be estimated based on half fracture length as follow:

$$S_{x} = \frac{1}{2\sqrt{\pi\eta_{x}t}}e^{-\frac{(x_{m}-x^{*})^{2}}{4\eta_{x}t}} = \frac{1}{2\sqrt{\pi\eta_{x}t}}\int_{-x_{f}}^{x_{f}}e^{-\frac{(x_{m}-x-x_{p})}{4\eta_{x}t}}dx_{p} = \frac{1}{2}\begin{bmatrix}erf\left(\frac{x_{m}-x+x_{f}}{2\sqrt{\eta_{x}t}}\right) - erf\left(\frac{x_{m}-x-x_{f}}{2\sqrt{\eta_{x}t}}\right) \\ erf\left(\frac{x_{m}-x-x_{f}}{2\sqrt{\eta_{x}t}}\right) \end{bmatrix}$$

$$(A-4)$$

$$= \frac{1}{2}\left[erf\left(\frac{x_{D}+1}{2\sqrt{t_{D}}}\right) - erf\left(\frac{x_{D}-1}{2\sqrt{t_{D}}}\right)\right]$$

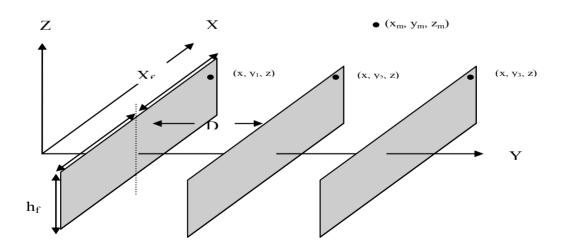


Figure A-2. The monitoring point and the source point of partially penetrating multiple transverse hydraulic fractures

 $S_{v}$  can be derived as follow:

$$S_{y} = \frac{1}{2\sqrt{\pi\eta_{y}t}}e^{-\frac{(y_{m}-y')^{2}}{4\eta_{t}}} = \frac{1}{2\sqrt{\pi\eta_{y}t}}\sum_{n=1}^{n=\infty}e^{-\frac{(y_{m}-y-nD)^{2}}{4\eta_{y}t}} = \frac{\sqrt{n_{x}/\eta_{y}}}{2\sqrt{\pi t_{D}}}\sum_{n=1}^{n=\infty}e^{-\frac{(y_{D}-nD_{D})^{2}}{4t_{D}}}$$
(A-5)

 $S_z$  represents the instantaneous source function that is affected by the height of the formation and the height of fractures as shown in Figure A-3. Gringarten and Ramey 1973 presented the solution for this source function as:

$$S_{z} = \frac{h_{f}}{h} \left[ 1 + \frac{4h}{\pi h_{f}} \sum_{N=1}^{N=\infty} \frac{1}{N} e^{-\frac{N^{2}\pi^{2}\eta_{z}t}{h^{2}}} \sin\left(N\pi \frac{h_{f}}{2h}\right) \cos\left(N\pi \frac{z_{f}}{h}\right) \cos\left(N\pi \frac{z}{h}\right) \right]$$
(A-6)

Substitute Eqs. (A-4), (A-5), and (A-6) in Equation (A-2) first and then substitute Eqs. (A-2) and (A-3) in Equation (A-1) gives:

$$\Delta P = \frac{qh_f}{8nx_f h_f \phi ch \sqrt{\pi \eta_y}} \int_0^t \frac{1}{\sqrt{t}} \left[ erf\left(\frac{x_m - x + x_f}{2\sqrt{\eta_x t}}\right) - erf\left(\frac{x_m - x - x_f}{2\sqrt{\eta_x t}}\right) \right]$$

$$\times \sum_{n=1}^{n=\infty} e^{-\frac{(ym - y - nD)^2}{4\eta_y t}} \times \left[ 1 + \frac{4h}{\pi h_f} \sum_{N=1}^{N=\infty} \frac{1}{N} e^{-\frac{N^2 \pi^2 \eta_z t}{h^2}} \sin\left(N\pi \frac{h_f}{2h}\right) \cos\left(N\pi \frac{z_f}{h}\right) \cos\left(N\pi \frac{z}{h}\right) \right] dt$$
(A-7)

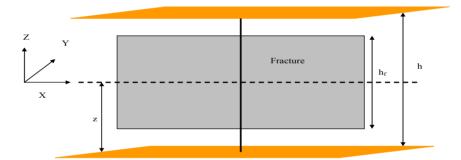


Figure A-3. Schematic diagram of partial penetrating hydraulic fracture

In dimensionless form, the final model for pressure response of horizontal wells intersecting by multiple partially penetrating vertical hydraulic fractures is:

$$P_{D} = \frac{\sqrt{\pi}}{4n} \int_{0}^{t_{D}} \frac{1}{\sqrt{t_{D}}} \left[ erf\left(\frac{x_{D}+1}{2\sqrt{t_{D}}}\right) - erf\left(\frac{x_{D}-1}{2\sqrt{t_{D}}}\right) \right] \times \sum_{n=1}^{n=\infty} e^{-\frac{(y_{D}-nD_{D})^{2}}{4t_{D}}} \times \left[ 1 + \frac{4}{\pi h_{hfD}} \sum_{N=1}^{N=\infty} \frac{1}{N} e^{-N^{2}\pi^{2}h_{yD}^{2}t_{D}} \sin\left(N\pi \frac{h_{hfD}}{2}\right) \cos\left(N\pi z_{fD}\right) \cos\left(N\pi z_{hfD}\right) \right] dt$$
(A-8)

where:

$$x_D = \frac{x_m - x}{x_f} \tag{A-9}$$

$$y_D = \frac{y_m - y}{x_f} \sqrt{\frac{k_x}{k_y}}$$
(A-10)

$$z_{fD} = \frac{z_f}{h} \tag{A-11}$$

$$h_{x/D} = \frac{x_f}{h} \sqrt{\frac{k_z}{k_x}}$$
(A-12)

$$z_{hfD} = \frac{z}{h} \tag{A-13}$$

$$h_{hfD} = \frac{h_f}{h} \tag{A-14}$$

$$D_D = \frac{D}{x_f} \sqrt{\frac{kx}{k_y}}$$
(A-15)

$$t_{D} = \frac{0.0002637k_{x}t}{\phi\,\mu\,cx_{f}^{2}} \tag{A-16}$$

$$P_D = \frac{2\pi \sqrt{k_x k_y} h \Delta P}{q \mu}$$
(A-17)

To solve the above model given in Equation (A-8), three long time approximations should be done based on the fluid flow dynamic and flow regimes in late time. The first approximation is for instantaneous source function  $S_x$  given by Equation (A-4).

$$erf\left(\frac{x_{D+1}}{2\sqrt{t_D}}\right) = \frac{2}{\pi} \sum_{n=0}^{n=\infty} \frac{(-1)^n}{n!} \frac{\left(\frac{x_{D+1}}{2\sqrt{t_D}}\right)^{2n+1}}{(2n+1)} = \frac{x_{D+1}}{\sqrt{t_D}} - \frac{(x_D+1)^3}{12t_D^{3/2}} + \frac{(x_D+1)^5}{160t_D^{5/2}} - \dots + \dots = \frac{x_D+1}{\sqrt{t_D}}$$
(A-18)

and:

$$erf\left(\frac{x_D-1}{2\sqrt{t_D}}\right) = \frac{2}{\pi} \sum_{n=0}^{n=\infty} \frac{(-1)^n}{n!} \frac{\left(\frac{x_{D11}}{2\sqrt{t_D}}\right)^{2n+1}}{(2n+1)} = \frac{x_{D11}}{\sqrt{t_D}} - \frac{(x_D-1)^3}{12t_D^{3/2}} + \frac{(x_D-1)^5}{160t_D^{5/2}} - \dots + \dots = \frac{x_D-1}{\sqrt{t_D}}$$
(A-19)

therefore:

$$t_D \ge \frac{25}{3} (xD+1)$$
 (A-20)

and:

$$t_D \ge \frac{25}{3} (xD - 1)$$
 (A-21)

The second approximation is for the instantaneous source function  $S_y$  given in Equation (A-5).

$$S_{y} = \frac{\sqrt{n_{x}/\eta_{y}}}{2\sqrt{\pi t_{D}}} \sum_{n=1}^{n=\infty} e^{-\frac{(y_{D}-nD_{D})^{2}}{4t_{D}}} = \frac{\sqrt{n_{x}/\eta_{y}}}{2\sqrt{\pi t_{D}}} \left[ 1 - \frac{(y_{D}-nD_{D})^{2}}{4t_{D}} + \frac{(y_{D}-nD_{D})^{4}}{32t_{D}^{2}} - \dots \right]$$
(A-22)

The exponential expansion can be approximated by its first term:

$$\frac{100(y_D - nD_D)^2}{4t_D} \le 1$$
 (A-23)

therefore:

$$t_D \ge 25(y_D - nD_D)^2$$
 (A-24)

The third approximation for the instantaneous source function  $S_z$  is given in Equation (A-6).

$$S_{z} = \frac{h_{f}}{h} \left[ 1 + \frac{4h}{\pi h_{f}} \sum_{N=1}^{N=\infty} \frac{1}{N} e^{-\frac{N^{2} \pi^{2} \eta_{z} t}{h^{2}}} \sin\left(N\pi \frac{h_{f}}{2h}\right) \cos\left(N\pi \frac{z_{f}}{h}\right) \cos\left(N\pi \frac{z}{h}\right) \right] =$$

$$\frac{h_{f}}{h} + \frac{4}{\pi} \sum_{N=1}^{N=\infty} \frac{1}{N} e^{-\frac{N^{2} \pi^{2} \eta_{z} t}{h^{2}}} \sin\left(N\pi \frac{h_{f}}{2h}\right) \cos\left(N\pi \frac{z_{f}}{h}\right) \cos\left(N\pi \frac{z}{h}\right)$$
(A-25)

Since:

$$\frac{4}{\pi}e^{-\pi^2 h_{yD}^2 t_D} \le 0.01 \tag{A-26}$$

therefore:

$$t_D \ge \frac{5}{\pi^2 h_{xD}^2} \tag{A-27}$$

The long time approximation can be written as:

$$P_{D} = \frac{q}{2nx_{f}h_{f}\theta\mu} \int_{0}^{t_{D1}} X(x_{D}, t_{D}) \times YZ(y_{D}, z_{D}, t_{D}, \phi_{v}, z_{fD}, h_{fD}, h_{D}) + \frac{1}{2} \int_{t_{D1}}^{t_{D}} \frac{1}{\tau_{D}} d\tau_{D}$$

$$= P_{D}(x_{D}, y_{D}, z_{D}, z_{wD}, L_{D}, t_{D1}) + \frac{1}{2} \ln(\frac{t_{D}}{t_{D1}})$$
(A-28)

and the proper time for this approximation is:

$$t_{D1} \ge \begin{bmatrix} \frac{25}{3} (xD + 1) \\ \frac{25}{3} (xD - 1) \\ 25 (y_D - nD_D)^2 \\ \frac{5}{\pi^2 h_{xD}^2} \end{bmatrix}$$
(A-29)

#### 2) Inclined Hydraulic Fractures:

For partially penetrating multiple inclined fractures as shown in Figure A-4, the model for pressure behavior can be derived using the same method as for the partially penetrating multiple vertical fractures, except the instantaneous source function in the vertical direction should be as:

$$S_{z} = \frac{h_{f}\cos(\theta_{v})}{h} \left[ 1 + \frac{4h}{\pi h_{f}\cos(\theta_{v})} \sum_{N=1}^{N=\infty} \frac{1}{N} e^{-\frac{N^{2}\pi^{2}\eta_{z}t}{h^{2}}} \sin\left(N\pi \frac{h_{f}\cos(\theta_{v})}{2h}\right) \cos\left(N\pi \frac{z_{f}}{h}\right) \cos\left(N\pi \frac{z_{f}}{h}\right) \right]$$
(A-30)

therefore the pressure model becomes:

$$\Delta P = \frac{qh_f}{8nx_f h_f \phi ch \sqrt{\pi\eta_y}} \int_0^t \frac{1}{\sqrt{t}} \left[ erf\left(\frac{x_m - x + x_f}{2\sqrt{\eta_x t}}\right) - erf\left(\frac{x_m - x - x_f}{2\sqrt{\eta_x t}}\right) \right] \times \sum_{n=1}^{n=\infty} e^{-\frac{(ym - y - nD)^2}{4\eta_y t}}$$

$$\times \left[ 1 + \frac{4h}{\pi h_f \cos(\theta_y)} \sum_{N=1}^{N=\infty} \frac{1}{N} e^{-\frac{N^2 \pi^2 \eta_z t}{h^2}} \sin\left(N\pi \frac{h_f \cos(\theta_y)}{2h}\right) \cos\left(N\pi \frac{z_f}{h}\right) \cos\left(N\pi \frac{z}{h}\right) \right] dt$$
(A-31)

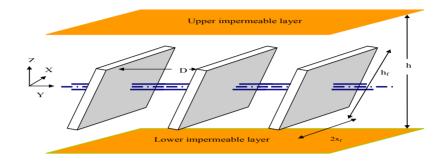


Figure A-4. Horizontal well intersected by partially penetrating multiple inclined hydraulic fractures

In dimensionless form, the model becomes:

$$P_{D} = \frac{\sqrt{\pi}}{4n} \int_{0}^{t_{D}} \frac{1}{\sqrt{t_{D}}} \left[ erf\left(\frac{x_{D}+1}{2\sqrt{t_{D}}}\right) - erf\left(\frac{x_{D}-1}{2\sqrt{t_{D}}}\right) \right] \times \sum_{n=1}^{n=\infty} e^{-\frac{(y_{D}-nD_{D})^{2}}{4t_{D}}} \times \left[ 1 + \frac{4}{\pi h_{hfD}\cos(\theta_{v})} \sum_{N=1}^{N=\infty} \frac{1}{N} e^{-N^{2}\pi^{2}h_{yfD}^{2}t_{D}} \sin\left(N\pi \frac{h_{hfD}\cos(\theta_{v})}{2}\right) \cos\left(N\pi z_{fD}\right) \cos\left(N\pi z_{hfD}\right) \right] dt$$
(A-32)

Appendix-B: Plots for Partially Penetrating Multiple Inclined Hydraulic Fractures

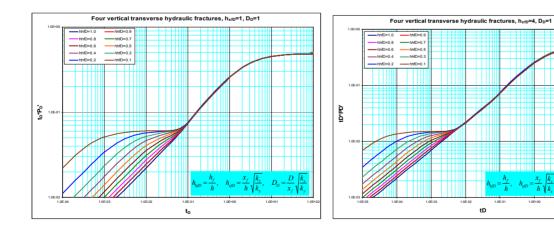


Figure B-5. Pressure and pressure derivative plot

Figure B-6. Pressure and pressure derivative plot

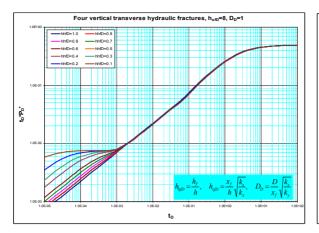


Figure B-7. Pressure and pressure derivative plot

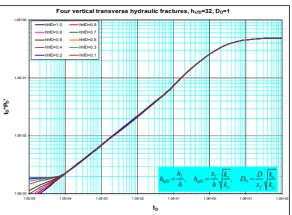


Figure B-8. Pressure and pressure derivative plot

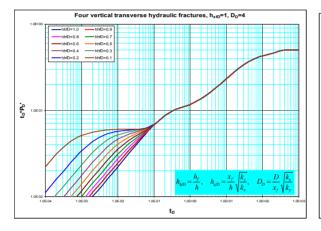


Figure B-9. Pressure and pressure derivative plot

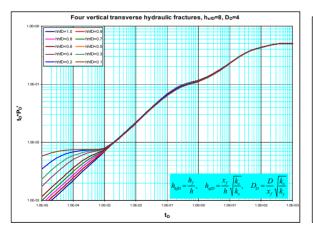


Figure B-11. Pressure and pressure derivative plot

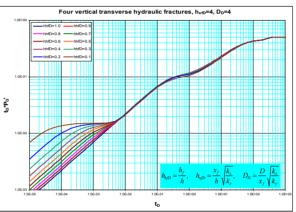


Figure B-10. Pressure and pressure derivative plot

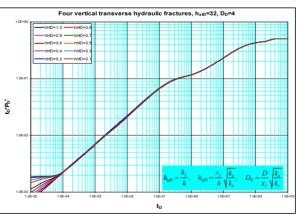


Figure B-12. Pressure and pressure derivative plot

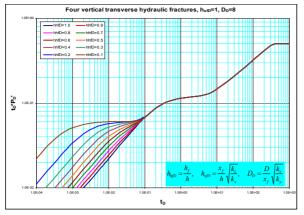


Figure B-13. Pressure and pressure derivative plot

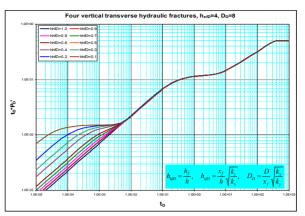


Figure B-14. Pressure and pressure derivative plot

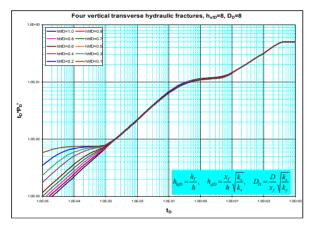


Figure B-15. Pressure and pressure derivative plot

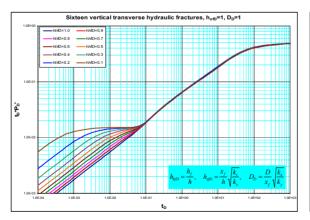


Figure B-29. Pressure and pressure derivative plot

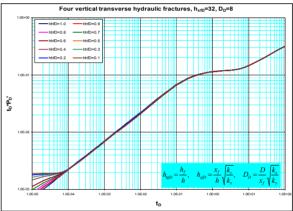


Figure B-16. Pressure and pressure derivative plot

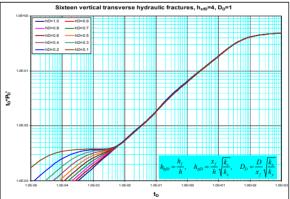


Figure B-30. Pressure and pressure derivative plot

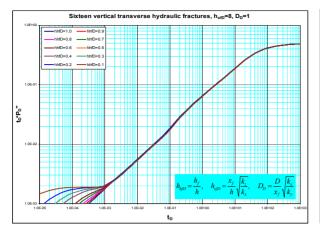


Figure B-31. Pressure and pressure derivative plot

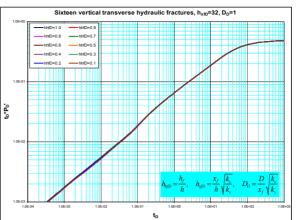


Figure B-32. Pressure and pressure derivative plot

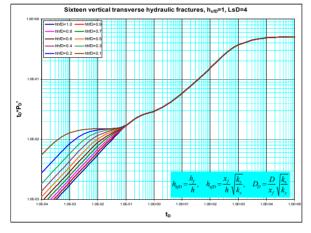


Figure B-33. Pressure and pressure derivative plot

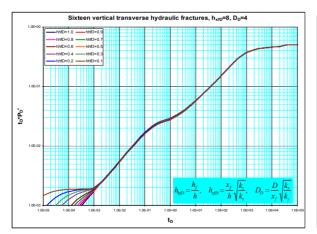


Figure B-35. Pressure and pressure derivative plot

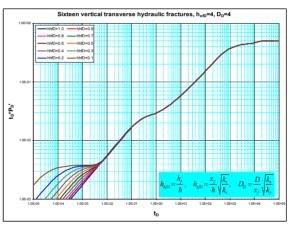


Figure B-34. Pressure and pressure derivative plot

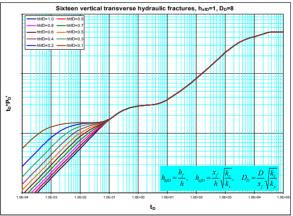


Figure B-36. Pressure and pressure derivative plot

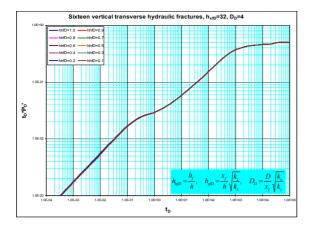


Figure B-37. Pressure and pressure derivative plot

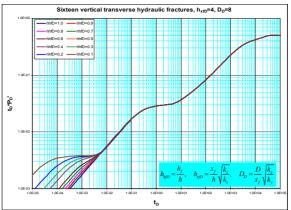


Figure B-38. Pressure and pressure derivative plot

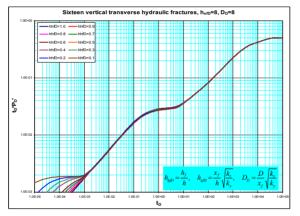


Figure B-39. Pressure and pressure derivative plot

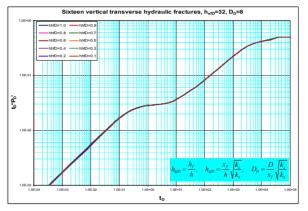


Figure B-40. Pressure and pressure derivative plot

# **Appendix-C: Tables**

Table C-1

t,hrs	Pwf, psi	t,hrs	Pwf, psi	t,hrs	Pwf, psi	t,hrs	Pwf, psi	t,hrs	Pwf, psi
0.000000	5000.00	0.000607	4997.70	0.1214	4985.77	18.20	4901.5	2427	4475.29
0.000006	4999.76	0.001214	4997.00	0.1820	4983.07	24.27	4892.8	3033	4432.96
0.000012	4999.66	0.00182	4996.56	0.2427	4980.8	30.34	4885.4	3640	4397.07
0.000018	4999.58	0.00243	4996.23	0.3034	4978.79	36.41	4878.9	4247	4365.94
0.000024	4999.52	0.0030	4995.98	0.3641	4976.98	42.47	4873.0	4854	4338.49
0.000030	4999.46	0.0036	4995.76	0.424	4975.33	48.54	4867.6	5460	4313.95
0.000036	4999.41	0.0042	4995.57	0.485	4973.79	54.61	4862.6	6067	4291.78
0.000043	4999.36	0.0049	4995.41	0.546	4972.36	60.68	4858.0	12135	4142.55
0.000049	4999.32	0.0055	4995.25	0.61	4971.01	121.3	4822.1	18202	4053.79
0.000055	4999.27	0.0061	4995.11	1.21	4960.61	182.0	4796.1	24270	3983.97
0.000061	4999.23	0.0121	4993.99	1.82	4953.41	242.7	4774.7	30337	3929.82
0.000121	4998.92	0.0182	4993.13	2.43	4947.9	303.3	4756.3	36405	3885.57
0.000182	4998.68	0.0243	4992.41	3.03	4943.44	364.0	4739.9	42472	3848.16
0.000243	4998.48	0.0303	4991.78	3.64	4939.7	424.7	4724.9	48540	3815.76

0.000303	4998.31	0.0364	4991.2	4.25	4936.48	485.4	4711.1	54607	3787.17
0.000364	4998.16	0.0425	4990.68	4.85	4933.64	546.0	4698.3	60675	3761.6
0.000425	4998.03	0.0485	4990.19	5.46	4931.1	606.7	4686.2		
0.000485	4997.91	0.0546	4989.73	6.07	4928.79	1213	4592.9		
0.000546	4997.80	0.0607	4989.29	12.1	4912.48	1820	4526.8		

Table C-2

t,hrs	Pwf, psi	t,hrs	Pwf, psi	t,hrs	Pwf, psi	t,hrs	Pwf, psi	t,hrs	Pwf, psi
0	10000.0	0.00077	9994.95	0.1553	9971.73	23.299	9479.96	3106	6668.39
7.77E-06	9999.47	0.0016	9993.35	0.233	9966.34	31.066	9391.53	3883	6510.57
1.55E-05	9999.25	0.0023	9992.35	0.311	9961.44	38.832	9314.31	4659	6381.28
2.33E-05	9999.09	0.0031	9991.61	0.388	9956.8	46.60	9245.3	5436	6271.79
3.11E-05	9998.94	0.0039	9991.03	0.466	9952.35	54.36	9182.67	6213	6176.88
3.88E-05	9998.82	0.0047	9990.55	0.544	9948.04	62.13	9125.24	6989	6093.16
4.66E-05	9998.71	0.0054	9990.14	0.621	9943.86	69.90	9072.15	7766	6018.29
5.44E-05	9998.6	0.0062	9989.77	0.699	9939.78	77.66	9022.76		
6.21E-05	9998.51	0.007	9989.45	0.777	9935.8	155.33	8657.22		
6.99E-05	9998.42	0.0078	9989.16	1.553	9900.11	232.99	8416.47		
7.77E-05	9998.33	0.0155	9986.99	2.33	9869.83	310.66	8236.67		
0.000155	9997.64	0.0233	9985.41	3.107	9843.21	388.32	8093.13		
0.000233	9997.12	0.0311	9984.09	3.883	9819.25	465.98	7973.71		
0.000311	9996.68	0.0388	9982.92	4.66	9797.32	543.65	7871.5		
0.000388	9996.3	0.0466	9981.86	5.436	9777	621.31	7782.17		
0.000466	9995.98	0.0544	9980.89	6.213	9757.99	698.98	7702.85		
0.000544	9995.68	0.0621	9979.98	6.99	9740.07	776.64	7631.51		
0.000621	9995.41	0.0699	9979.13	7.766	9723.09	1553.28	7154.65		
0.000699	9995.17	0.0777	9978.33	15.533	9585.47	2329.92	6871.03		